

STRUCTURAL, CONDUCTIVITY AND SPECTROSCOPIC ASPECTS OF ONE-DIMENSIONAL TRANSITION METAL COMPLEXES

JOHN R. FERRARO*

Department of Chemistry, Loyola University, Chicago, Illinois 60626 (U.S.A.)

CONTENTS

| | |
|---|-----|
| A. Introduction | 205 |
| B. Discussion | 206 |
| (i) Predominantly square-planar organometallic 1-D tetracyanoplatinates | 209 |
| (ii) Planar organometallic complexes | 211 |
| (iii) Non-planar organometallic complexes | 215 |
| (iv) Spectroscopic studies | 217 |
| C. Summary | 228 |
| D. Structures for organometallic complexes | 230 |
| Acknowledgements | 230 |
| References | 230 |

A. INTRODUCTION

The quest for materials with unusual semiconducting and conducting properties has provided impetus for research in the area of “linear chain” or “pseudo-one-dimensional” compounds. These are materials which, by virtue of their crystalline packing arrangements, exhibit anisotropy in certain intensive variables including electrical, optical and magnetic behavior. Three broad categories can be defined for compounds comprising the area of electrical conduction: (1) organic donor–acceptor complexes such as tetra-thiofulvalenium-7,7,8,8-tetracyano-*p*-quinodimethanide (TTF–TCNQ), (2) polymeric systems, i.e. polysulfurnitride (SN)_x, and (3) transition metal complexes. Square-planar coordination complexes, which are included the third category, have been extensively studied with respect to their unidimensional characteristics. The results indicate that these compounds can be divided into three classes which are the subject of this review.

* Searle professor of chemistry.

Perhaps the most avidly studied anisotropic transition metal complexes are the partially oxidized, predominantly square-planar, tetracyanoplatinates [1,2]. These are appropriately classified as organometallic compounds due to the presence of metal-carbon σ bonds. These materials exhibit anisotropic physical properties, with the most important being the 1-D metallic conductivity along the metal chain axis. Recent investigations have demonstrated that high conductivities and anisotropic properties can also be obtained for complexes of transition metals with larger, more complex macrocyclic ligand systems. In particular, highly planar, organic ligands such as phthalocyanine [3,4] and tetrabenzporphyrin [5] have been shown to form transition metal complexes which are anisotropically conducting materials when oxidized by iodine [3-5]. Other pseudo-macrocyclic systems such as the bis(glyoximates) can also, with certain transition metals, be partially oxidized by I_2 to form complexes with enhanced conductivities as contrasted to their unoxidized forms [6-10]. These compounds, unlike the phthalocyanines, are not strictly planar, particularly in the ligand periphery.

Thus, the cycle of square-planar coordinated transition metal complexes ranges from the predominantly planar organometallic to the strictly planar, expanded ligand system, organometallic, to the non-planar expanded ligand, organometallic compounds. This review deals mainly with the structural influences on one dimensionality, and the effect of various steric and electronic factors on the formation of highly conducting systems. The importance of spectroscopy in elucidating the nature of these complexes is discussed. Aspects such as temperature dependencies and magnetic behavior are not discussed.

B. DISCUSSION

Several aspects of one dimensionality and the highly conducting systems should be considered before examining the three classes of transition metal complexes.

(1) Mixed valency. The electrical properties of a solid are determined to a large extent by its electronic energy levels, their occupation and the gaps between them. According to Band Theory when N atoms are brought together so also are N molecular orbitals covering a range of orbital energies of finite width. At indefinitely large values of N these energies can be considered to form a continuous band. Metallic conduction results from the presence of partially filled bands in which electrons can be readily excited to unfilled orbitals close in energy ($E \ll kT$) to the highest filled orbital, the result being electron mobility and electrical conduction. The presence of non-integral oxidation states and hence the creation of partially filled bands thus becomes an important factor in the creation of highly conducting

systems. The theory behind charge transport has been treated in detail elsewhere [11–13]. Briefly, in systems with integral oxidation states charge is mobilized through the creation of states in which positive and negative ions are separated along the chain, while partially oxidized systems already have holes which have been formed as a result of fractional oxidation. In order for the former to occur, a large activation energy is required. In the latter, however, charge transport can readily occur by movement of the holes between degenerate configurations.

(2) Steric aspects. For strong intermolecular interactions to occur, close molecular approach is a necessity. One way to facilitate this is accomplished by square-planar coordination about the metal ion, and by using planar ligand systems. (In the transition metal area efforts to achieve 1-D chains by using binuclear complexes M_2L_6 or M_2L_4 have not been as successful). Short metal–metal distances that are only 0.1 to 0.3 Å longer than those in the parent metal have been obtained in the partially oxidized square-planar tetracyanoplatinates by premeditated design [14]. Even for organic molecular metals, a criterion for creating conductive molecular crystals is that the parent compound be a planar complex of metal and ligand [15,16]. The logic behind employing planar systems is evident. Bulky ligands or molecules, while perhaps capable of stacking closely, may not approach each other due to steric repulsions. On the other hand some complexes which show relatively large distortions from planarity have been found to exhibit unexpectedly large conductivities. The partially oxidized octamethyltetrabenzoporphinatonicel(II), $Ni(OMTBP)I$, is a case in point [16]. In fact, the nickel and palladium bis(diphenylglyoximates), despite the bulky phenyl substituents, display higher conductivities in their partially oxidized form than the corresponding more planar bis(benzoquinonedioximates). These compounds are discussed in greater detail in section (iii).

Given that square-planar geometry is a desirable characteristic in 1-D transition metal complexes, an investigation into the propensity of various metals for forming this geometry is appropriate. Krogmann has pointed out that metals having accessible d^8 electron configuration have a greater tendency to form square-planar coordinated complexes which stack to form columnar structures [1]. Table I lists metals with accessible d^8 electron configurations. Presently only Pt, Ir, and Rh (in decreasing order of occurrence) have been observed to form 1-D metal chain structures with extremely short metal–metal separations. The compounds formed from zero-valent states of Fe, Ru, and Os favor trigonal-bipyramidal geometries or clusters which tends to prevent chain formation and hence extended metal–metal interactions.

(3) Electronic considerations are also of major importance as can be seen by examining the capacity of the d^8 metals for forming highly conducting

TABLE I

Metals with accessible d^8 electron configurations

| Configuration | Metal (oxidation state) | | | |
|---------------|-------------------------|--------|--------|--------|
| $3d^8$ | Fe(0) | Co(+1) | Ni(+2) | Cu(+3) |
| $4d^8$ | Ru(0) | Rh(+1) | Pd(+2) | Ag(+3) |
| $5d^8$ | Os(0) | Ir(+1) | Pt(+2) | Au(+3) |

1-D systems. If, as is often the case in transition metal complexes, the intermolecular interaction involves overlapping d orbitals, orbital spatial extension is a major consideration. Due to $5d > 4d > 3d$ orbital extension the most highly conducting complexes would be expected for third row transition metals. Thus both Pt^{2+} and Ir^+ form complexes which exhibit metallic conduction, but Au^{3+} does not, due to a contracted $5d$ orbital as a result of higher effective charge. Accordingly, Ni^{2+} and Pd^{2+} would be expected to form complexes exhibiting lower conductivities. This is observed in 1-D systems where d orbital interaction is the major contributing mechanism of conduction. For organic moieties where p_z orbital interactions become important a similar reasoning would suggest that the heavier Group 4 elements such as Si would be a better choice in synthesizing organic 1-D compounds, all other aspects being equal. The widely differing chemistry of Si and other Group 4 elements, compared to C, makes it difficult to prove this assertion, however.

(4) Ligand system. The small, non-bulky ligands which promote a planar configuration and have the correct steric requirements to allow close stacking are limited and mainly involve CN^- , CO, and oxalate $(C_2O_4)^{2-}$. NH_3 offers steric problems, S^{2-} appears to be too large and F^- does not combine with transition metals in their low oxidation states. The complexes formed with the expanded ligand systems, while sometimes highly conducting, do not exhibit the close intermolecular spacings readily accessible with the less bulky systems. Even in the more congested, extended ligand systems, as long as steric repulsions are minimized, close intermolecular approach should be allowed by snugly fitting the complexes to each other. In general, however, while intermolecular distances in the partially oxidized tetracyanoplatinates are on the order of 2.9 Å or even less, the analogous phthalocyanato systems exhibit spacings of 3.2 Å or longer. The mode of conduction, whether via primarily d -character orbitals, as in the former, versus ligand-centered conduction in the latter, may also influence the packing of the molecules. Evidently d orbital interactions necessitate closer approach, at least on the

basis of the experimental evidence cited in the subsequent sections.

The three main classes of transition metal complexes exhibiting square-planar coordination and anisotropic behavior are discussed in greater detail below.

(i) Predominantly square-planar organometallic 1-D tetracyanoplatinates

Oxidation of $\text{Pt}(\text{CN})_4^{2-}$ results in the formation of complexes with metallic gold, bronze or copper colors [1,2]. Although a metallic luster does not always signify metallic behavior, in this case the resulting complexes are characterized by anisotropic electrical, magnetic, and optical properties. In particular, electrical conductivity along the metal chain and insulating behavior in orthogonal directions are observed. Conductivities along the Pt–Pt chain increase by $\sim 10^{10}$ from $5 \times 10^{-7} \Omega^{-1} \text{cm}^{-1}$ in the unoxidized $\text{K}_2\text{Pt}(\text{CN})_4 \cdot 3\text{H}_2\text{O}$ to a range of 0.5 to $2100 \Omega^{-1} \text{cm}^{-1}$ in the oxidized forms [2,11]. Also in conjunction with oxidation the Pt–Pt distances along the chain decrease from 3.478 Å in $\text{K}_2\text{Pt}(\text{CN})_4 \cdot 3\text{H}_2\text{O}$ to less than 2.95 Å [2,11]. A perspective view of the unit cell of $\text{Rb}_2\text{Pt}(\text{CN})_4(\text{FHF})_{0.40}$ is illustrated in Fig. 1.

The mechanism of conduction in these complexes is metal-centered involving electron delocalization along overlapping d_z^2 orbitals of the platinum. Partial oxidation is achieved by inclusion of small amounts of anion (e.g. Br^- , Cl^- , F^- , HF_2^- , $\text{Br}^- \text{Cl}^-$, $\text{O}_3\text{SOHOSO}_3^{3-}$, N_3^- , ClO_4^-) or by making the cation deficient [17] (K^+ , Rb^+ , Cs^+ , NH_4^+ , and the guanidinium are typical cations). The anion-deficient tetracyanoplatinates display somewhat

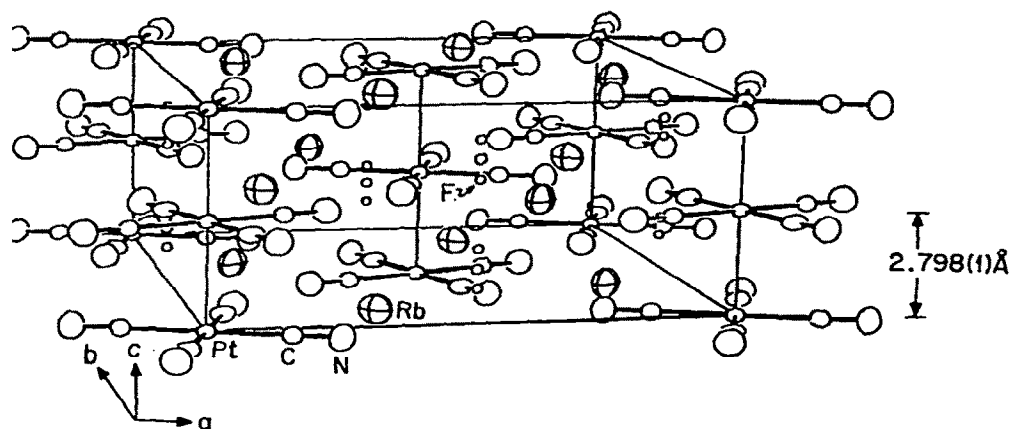


Fig. 1. A perspective view of the unit cell of $\text{Rb}_2[\text{Pt}(\text{CN})_4][\text{FHF}]_{0.40}$ [18]. Partially occupied fluorine positions are indicated by small circles. Permission granted by the N.Y. Academy of Sciences and authors.

higher conductivities than the cation-deficient types. Among the anion-deficient salts two structural types exist (primitive and body centered lattices). The hydrated salts form the primitive tetragonal lattices ($P4mm$) with M^+ cations in one-half of the unit cell and water molecules in the other half. The anhydrous salts are body-centered tetragonal ($I4/mcm$) and the cations occupy sites in the same plane as the $Pt(CN)_4^{2-}$ groups. The tendency toward hydration in the Krogmann salts is found to depend on both cation and anion. Large disparities in anion/cation size generally promote hydration; for example, in $Rb_2Pt(CN)_4Cl_{0.3}$ $r_{Rb^+}/r_{Cl^-} = 0.31$ and the result is a hydrated complex; in $Cs_2Pt(CN)_4Cl_{0.3}$ $r_{Cs^+}/r_{Cl^-} = 0.93$ and the resulting complex is anhydrous [18].

The intrachain and interchain Pt–Pt spacings in these compounds depend in part on the cation and anion size. An increase in cation and anion size has been observed to result in an increase in these distances according to X-ray crystallographic studies as shown in Table 2 [19]. Also, it would appear that as the degree of partial oxidation increases the inter- and intra-chain distances decrease, with a concomitant increase in electrical conductivity (Table 2).

With a decrease in temperature the conductivity along the Pt–Pt chain decreases [20]. This involves an interchain Coulombic interaction between the 1-D lattices causing the chains to undergo a 3-D ordering transition at T_{3D} . This could ultimately lead to a transition from a metal to a band semiconductor insulator. For any conductor a temperature T_p exists, which is defined as the mean field Peierls transition temperature for a one-dimensional lattice. The interchain coupling parameter, η , is measured by the ratio

TABLE 2

Comparison of DPO, intra- and inter-chain Pt–Pt Spacings and interchain coupling parameter for several 1-D tetracyanoplatinates

| Compound | DPO ^a | Pt–Pt (intra) (Å) | Pt–Pt (inter) (Å) | η ^b |
|---------------------------------------|------------------|-------------------------|-------------------------|---------------------|
| $K_2[Pt(CN)_4]Cl_{0.3} \cdot 3 H_2O$ | 2.3 | 2.87 | 9.883 | 0.019 |
| $Rb_2[Pt(CN)_4]Cl_{0.3} \cdot 3 H_2O$ | 2.3 | 2.90 | 10.142 | 0.022 |
| $K_2[Pt(CN)_4]Cl_{0.3} \cdot 3 H_2O$ | 2.3 | 2.87 | 9.883 | 0.019 |
| $K_2[Pt(CN)_4]Br_{0.3} \cdot 3 H_2O$ | 2.3 | 2.88 | 9.907 | 0.021 |
| $Cs[Pt(CN)_4]Cl_{0.30}$ | 2.30 | 2.859 | 9.317 | 0.017 |
| $Cs[Pt(CN)_4][FHF]_{0.39}$ | 2.39 | 2.833 | 9.233 | 0.017 |

^a Degree of partial oxidation.

^b $\eta = T_{3D}/T_p$ = interchain coupling parameter (ref. 20).

T_{3D}/T_p , and depends in part on the extent of hydrogen bonding between Pt atom chains (see Table 2) [20]. The results for the primitive (p) and body-centered tetragonal (i) anion-deficient tetracyanoplatinates are similar. However, the decrease in conductivity is more pronounced for $K_2Pt(CN)_4 \cdot Cl_{0.3} \cdot 3H_2O$ (p) than in the salts involving the $(FHF)^-$ anion (i). A larger and more easily polarized Cl^- provides a more effective interchain coupling mechanism than $(FHF)^-$. Thus, the anion also plays an important role in the coupling mechanism. Since T_{3D} is a measure of Coulombic interchain coupling, and is in part dependent on hydrogen bonding, it is found that T_{3D} and consequently η are lower in the anhydrous salts than for the hydrated compounds.

Another consideration which is important to the anion-deficient partially oxidized tetracyanoplatinates (POTCP) salts is the possibility of chain dimerization occurring [20]. $Rb_2[Pt(CN)_4]Cl_{0.3} \cdot 3H_2O$ and several other p-type salts exhibit this behavior [20]. The dimerization decreases with a lowering of temperature. The degree of dimerization depends on the size of the cation (R^+). As R^+ increases the dimerization increases; for a given R^+ , as the Pt–Pt distances decrease the dimerization decreases. Since Pt–Pt distances are related to the degree of partial oxidation (DOP), the degree of dimerization is indirectly related to DOP.

For the cation-deficient POTCP salts optical reflection studies have demonstrated the 1-D metal nature of these substances [20]. Neutron scattering methods have indicated the presence of a Kohn anomaly. Additionally, it has been shown that $K_{1.75}[Pt(CN)_4] 1.5H_2O$ has a superlattice. The electrical conductivity behavior of $K_{1.75}[Pt(CN)_4] 1.5H_2O$ [Kdef(TCP)] is thus considerably different than that for $K_2[Pt(CN)_4]Br_{0.3} \cdot 3H_2O$ (KCP) where KCP is several orders of magnitude more conductive than Kdef(TCP). The differences are magnified by the fact that Kdef(TCP) demonstrates a Peierls transition as well as a non-Peierls distortion. In addition the presence of less water molecules in the Kdef(TCP) salts effects the intrachain interaction, inasmuch as η is very low for the Rbdef and Kdef(TBP) salts.

Further information concerning structural concepts and conductivities of partially oxidized tetracyanoplatinates (POTCP) is summarized in Table 3. For further discussion on these conductors see a recent review [20].

(ii) Planar organometallic complexes

The possibility of attaining highly conducting 1-D transition metal complexes with extended, higher molecular weight ligands was only recently realized. Phthalocyanines (Pc) and tetrabenzporphyrins were found to form highly conducting 1-D systems upon I_2 oxidation. A variety of transition metals were found to take part in this reaction including Fe(II), Co(II),

TABLE 3
Crystal structure and conductivities for several Krogmann-type conductors^a

| Conductor | Space group ^b | d_{Pt-Pt} (Å) (298 K) | Conductivity ^c (ohm cm) ⁻¹ | Color |
|---|--------------------------|-------------------------|--|-----------------|
| Pt metal | | 2.775 | 9.4×10^4 | Metallic |
| $K_2[Pt(CN)_4]Br_{0.30} \cdot 3 H_2O$ | $P4mm$ | 2.89 | 4–1050 | Bronze |
| $K_2[Pt(CN)_4]Cl_{0.30} \cdot 3 H_2O$ | $P4mm$ | 2.87 | ~200 | Bronze |
| $K_2[Pt(CN)_4]Br_{0.15}Cl_{0.15} \cdot 3 H_2O$ | $P4mm$ | | | |
| $Rb_2[Pt(CN)_4]Cl_{0.30} \cdot 3 H_2O$ | $P4mm$ | 2.877, 2.924 | 10 | Bronze |
| $Cs_2[Pt(CN)_4]Cl_{0.30}$ | $I4/mcm$ | 2.859 | ~200 | Bronze |
| $(NH_4)(H_3O)_{0.17}[Pt(CN)_4]Cl_{0.42} \cdot 2.83 H_2O$ | $P4mm$ | 2.910, 2.930 | 0.4 | Bronze |
| $Cs_2[Pt(CN)_4](N_3)_{0.25} \cdot 0.5 H_2O$ | $P4h2$ | 2.877 | | Reddish copper |
| $Rb_3(H_3O)_{0.4}[Pt(CN)_4][O_3SO \cdot H \cdot OSO_3]_{0.49} \cdot H_2O$ | $P\bar{1}$ | 2.826 | | Copper |
| $K_{1.75}[Pt(CN)_4] \cdot 1.5 H_2O$ | $P\bar{1}$ | 2.965, 2.961 | 115–125 | Bronze |
| $Rb_{1.75}[Pt(CN)_4] \cdot 1.5 H_2O$ | d | 2.94 | 1 | Bronze |
| $Cs_{1.75}[Pt(CN)_4] \cdot 1.5 H_2O$ | d | | | Bronze |
| $K_2[Pt(CN)_4](FHF)_{0.30} \cdot 3 H_2O$ | $P4mm$ | 2.918, 2.928 | | Reddish bronze |
| $Rb_2[Pt(CN)_4](FHF)_{0.40}$ | $I4/mcm$ | 2.798 | 2300 | Gold |
| $Rb_2[Pt(CN)_4](FHF)_{0.26} \cdot 1.7 H_2O$ | $C2/c$ | 2.89 | | Greenish bronze |
| $Cs_2[Pt(CN)_4](FHF)_{0.39}$ | $I4/mcm$ | 2.833 | 1600 | Reddish gold |
| $Cs_2[Pt(CN)_4](FHF)_{0.23}$ | $I4/mcm$ | 2.872 | 250–350 | Reddish bronze |
| $Cs_2[Pt(CN)_4]F_{0.19}$ | $Immm$ | 2.886 | | Reddish gold |
| $[C(NH_2)_3]_2[Pt(CN)_4](FHF)_{0.26} \cdot x H_2O$ | | 2.90 | | Bronze |
| $[C(NH_2)_3]_3[Pt(CN)_4]Br_{0.25} \cdot H_2O$ | $I4cm$ | 2.908 | | Bronze |

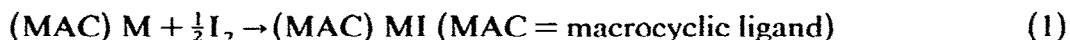
^a Data taken in part from ref. 17.

^b For the space group $P4mm$ the Pt–Pt intrachain distances are not required to be equal, but often appear to be so. When they have been determined to be different both distances are tabulated.

^c Results are for a range of literature values for room temperature and by the four-point-probe d.c. conductivity method.

^d The crystal class is monoclinic but the space group is unknown. The lattice constants for the Cs salt are $a = 18.35$, $b = 5.760$, $c = 19.92$ Å, $\beta = 109.03^\circ$; for the Rb salt the lattice constants are $a = 10.56$, $b = 33.2$, $c = 11.74$ Å, $\beta = 114.23^\circ$.

Ni(II), Cu(II), Zn(II), and Pt(II) according to eqn. (1) [3–5].



Notable about this series is the occurrence of first row transition metals not of d^8 configuration. This aspect, along with the observation that the metal-free phthalocyanine exhibits analogous behavior, suggests that a different mechanism of electrical conduction other than that observed for the tetracyanoplatinates is in effect. Both resonance Raman and ^{129}I Mössbauer studies indicate the form of the iodine to be mainly I_3^- with negligible amounts of I^- and I_2 , and can be formulated for the Ni complex as $[\text{NiPc}](\text{I}_3)_{0.33}$. EPR spectra indicate $g_{\parallel} = 2.012$ and $g_{\perp} = 2.006$ with a narrow line width, $W_{\text{pp}} = 5$ G. Such values are analogous to those found in π -cation radical type species and are indicative of ligand oxidation. The conductivity of the complexes at room temperature range from 250 to 600 $\Omega^{-1} \text{cm}^{-1}$ and are comparable to those of the purely organic metals TTF–TCNQ [4]. Temperature-dependence studies confirm the metallic conductivity of these systems. As the temperature is lowered, a metal–semiconductor transition occurs at ca. 55 K.

In systems such as the phthalocyanines, where a large cross sectional area is encountered, it becomes important to examine individual charge carriers and the mean free path of a carrier along a stacking direction [4,5]. The conductivity (σ) along the chain related to A , the cross sectional area, and λ , the mean free path becomes

$$\sigma = 2e^2\lambda/\pi hA$$

where e = electronic charge and h = Planck's constant/ 2π . For $[\text{NiPc}](\text{I}_3)_{0.33}$, λ ranges from 1.0 to 2.3 intermolecular spacings. This compares to 0.6 for $\text{K}_2\text{Pt}(\text{CN})_4\text{Br}_{0.3} \cdot 3\text{H}_2\text{O}$ and 0.4 to 0.6 for TTF–TCNQ although some of the highly conductive purely organic “metals” have considerably larger mean free paths such as 2.1 to 2.8 spacings for tetrathiatetracene triiodide. For nickel metal the mean free path is 24.

The structural aspects of the partially oxidized phthalocyanines can be examined from data on $[\text{NiPc}](\text{I}_3)_{0.33}$. Partially oxidized nickel tetrabenzoporphyrin can also be considered at this point since it behaves similarly to partially oxidized nickel phthalocyanine. Both have similarly shaped ligands, Ni–Ni spacings of ~ 3.25 Å, and indistinguishable structures [5]. Powder diffraction studies of other phthalocyanines MPcI_x and PcH_2I_x indicate similar structures. As is often the case with 1-D complexes, NiPcI crystallizes in the tetragonal space group ($P4mcc$). The cations and anions are stacked along the c axis. Figure 2 shows a perspective view down the c axis of the unit cell of $[\text{NiPc}](\text{I}_3)_{0.33}$. Phthalocyanine groups along the chain are staggered by 39.5° from adjacent neighbors. Intermolecular phtha-

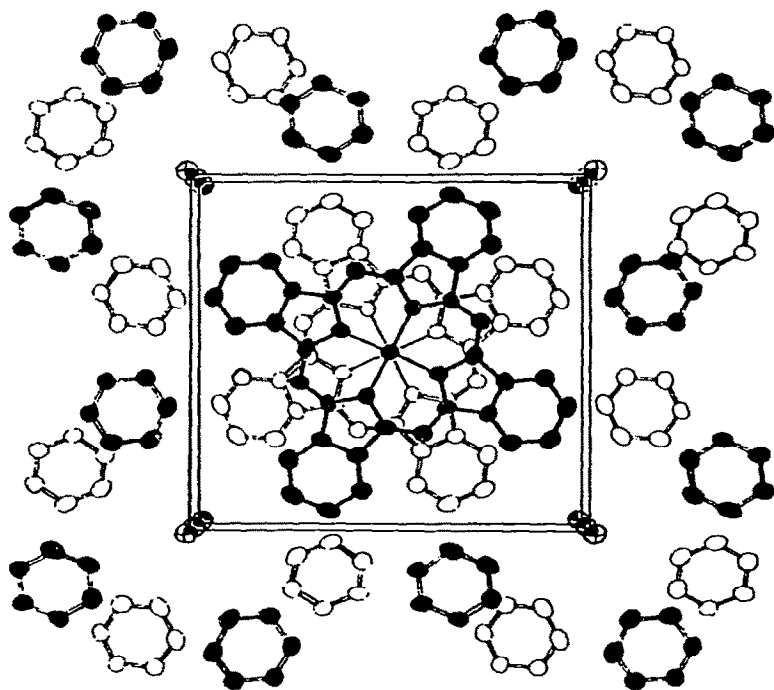


Fig. 2. View down the c axis of the unit cell of $[\text{NiPc}](\text{I}_3)_{0.33}$ [21]. Permission granted by the N.Y. Academy of Sciences and authors.

locyanine contacts along the chain direction are $3.244(3) \text{ \AA}$ [21a,21b]. Such a repeat distance would be considered large for $d_{\pi-\pi}$ interaction, but both the EPR data and the broad range of metals which are capable of forming these complexes indicate that ligand π -orbital interactions are undoubtedly the major mechanistic contributors to the conductivity.

More recently a new series of 1-D phthalocyanine complexes has been reported. These are polysiloxane, polygermyloxane and polystannyloxane complexes of phthalocyanine [22], which, although not of transition metals, should be mentioned. Upon I_2 oxidation these complexes form a wide range of dopant geometries. Resonance Raman measurements have shown the presence of I_3^- and no significant I_2 concentration. Large increases in electrical conductivity occur upon I_2 oxidation in the order $\sigma_{\text{Si}} \gtrsim \sigma_{\text{Ge}} > \sigma_{\text{Sn}}$. Powder diffraction studies show a tetragonal system with probably interplanar spacings of $3.33(2)$, $3.51(2)$ and $3.95(2) \text{ \AA}$, respectively, for Si, Ge and Sn. Again the mechanism of conductivity would appear to be via ligand interactions and so, undoubtedly, the variation in the conductivities of this series is due to the different interplanar spacings.

(iii) *Non-planar organometallic complexes*

A series of ligands of varying degrees of planarity comprises this group of compounds. Slight distortions from planarity are exemplified by the pseudo-macrocyclic bis(glyoximates) such as bis(diphenylglyoximate) nickel(II) and palladium(II) [6–10]. In general, the complexes are insulators with $\sigma \sim 10^{-12} \Omega^{-1} \text{ cm}^{-1}$ in their unoxidized form, and upon reaction with I_2 conductivity increases to the semiconductor range by a factor of $\sim 10^6$. For the partially oxidized bis(glyoximate) systems it would appear that only the Ni(II) and Pd(II) analogues form the partially oxidized complexes upon oxidation. The Pt(II) complexes are oxidized to Pt(IV). Conductivities for the unoxidized and oxidized complexes are shown in Table 3.

Structurally, the bis(glyoximates) are more analogous to the phthalocyanine complexes than the tetracyanoplatinates. In the metal bis(diphenylglyoximates) (dpg), square-planar columns (staggered by 90°) are formed with disordered chains of iodine in channels parallel to the metal chains, surrounded by phenyl groups [23,24]. A perspective view down the c axis of the unit cell of the $\text{Ni}(\text{dpg})_2(\text{I})$ is illustrated in Fig. 3. The iodine exists as the I_5^- ion, based on Raman and Mössbauer data. In the Ni compound the $\text{Ni}(\text{dpg})_2$ units are considered to be in a fractional oxidation state of +0.2.

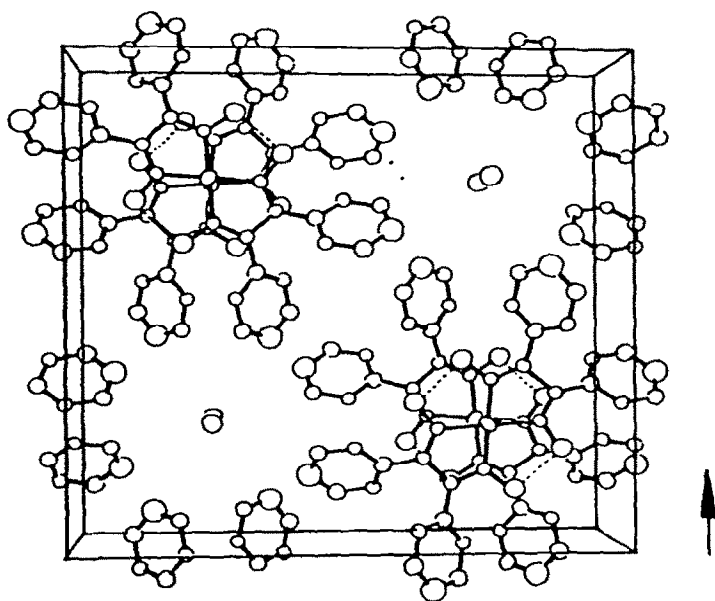


Fig. 3. Perspective view down the c axis of the unit cell of $[\text{Ni}(\text{dpg})_2](\text{I}_5)_{0.2}$. Dotted lines show the diphenylglyoximate O–H–O bonds [21,23,24]. Permission granted by the American Chemical Society and authors.

and the Ni–Ni distances are reduced from 3.547 Å in the non-oxidized state, to 3.223 Å in the oxidized version. The compound is formulated as $\text{Ni}(\text{dpg})_2(\text{I}_5)_{0.2}$. The bis(benzoquinone)dioximates (bqd) are closely related to the diphenylglyoximates [25a]. Stacks are found in the Pd compound, staggered by 65° and disordered chains of iodine in the chain direction. Pd–Pd distances are 3.184 Å in the oxidized form and 3.202 Å in the unoxidized form. The $\text{Pd}(\text{bqd})_2$ units carry a residual +0.17 fractional charge. A 10^3 to 10^4 fold increase in electrical conductivity occurs upon oxidation but still the conductivities are in the semiconductor range. The iodine is found to be in the form of the I_3^- ion.

In reviewing the dpg conductor in this class, we observe very little change occurring in conductivities and M–M distances as the metal changes (e.g. $\text{Ni} \rightarrow \text{Pd}$). Polyiodides are considered to play only a minor role in charge transport. Compounds containing no metal but polyiodide chains demonstrate low conductivities. Also, $\text{M}(\text{dpg})_2\text{Br}$ complexes show conductivities which are nearly identical to the $\text{M}(\text{dpg})_2(\text{I}_5)_{0.2}$ conductors. It is thus presently considered that the π systems in the ligand columns are the pathway for electrical conduction. Similar considerations can be made in the bis(benzoquinone)dioximate complexes.

Partially oxidized 1,4,5,8,9,12,13,16-octamethylbenzporphyrinatonickel(II), $\text{Ni}(\text{OMTBP})(\text{I}_3)_{0.36}$ has been recently structurally characterized by X-ray studies [16]. Methyl substitution of TBP increases the Ni–Ni spacing to ~ 3.77 Å from ~ 3.25 Å in the unsubstituted derivative. The room-temperature conductivity is $\sim 10 (\Omega \text{ cm})^{-1}$, a value less than that of $\sim 350 (\Omega \text{ cm})^{-1}$ for the unmethylated complex $\text{Ni}(\text{TBP})(\text{I}_3)_{0.33}$ [5]. $\text{Ni}(\text{OMTBP})(\text{I}_3)_{0.36}$ crystallizes in the space group $D_{4h}^{11}-P4/nbc$ of the tetragonal system with four formula units per cell. The structure consists of ruffled macrocycles stacked with relatively large intermolecular spacings along the c axis [$\text{Ni}-\text{Ni} = 3.778(5)$ Å]. Chains of severely disordered linear I_3^- units are parallel to the stacking axis between adjacent macrocycle columns. Metal–metal spacings do play a major role in the achievement of highly conducting systems; however, at least in the case of ligand-based conductors, the degree of partial oxidation appears to be a predominant factor. The $\text{Ni}(\text{OMTBP})(\text{I}_3)_{0.36}$ complex is, as expected from the longer metal–metal spacings, less highly conducting than its parent $\text{Ni}(\text{TBP})(\text{I}_3)_{0.33}$. The fact that it displays an unexpectedly large conductivity in the metallic range, despite its unfavorable stacking distances, must rest with the aspect of non-integral oxidation states.

Another class of electrically conductive metallomacrocycles doped with iodine has recently been synthesized [25b]. These are the metallodihydrodi-benzo[b,i][1,4,8,11]tetraazacyclotetradecine complexes. The hydrogen substituted ligands are abbreviated taa, while the methylated ligands are designated tmtaa. Raman spectra of $[\text{Ni}(\text{taa})][\text{I}_{1.80}]$ and $[\text{Ni}(\text{tmtaa})][\text{I}_{2.44}]$ exhibit

typical I_3^- scattering patterns (vibrations at 108 cm^{-1}). The charge distribution may be represented as $[Ni(taa)]^{0.6+}[I_3^-]_{0.6}$ and $[Ni(tmtaa)]^{0.8+}[I_3^-]_{0.8}$. ESR data support the notion that the oxidation involves MOs which are predominantly ligand-centered, producing a π -radical cation-hole as has been invoked for the iodinated phthalocyanines and porphyrins. An increase by a factor of ca. 10^{15} in the σ conductivity $(\text{ohm cm})^{-1}$ is observed in going from $Ni(taa)$ to $[Ni(taa)][I_3]_{0.6}$ and $Ni(tmtaa)$ to $[Ni(tmtaa)][I_3]_{0.8}$. A somewhat lower increase in conductivity is observed for the Co and Cu analogues.

More drastic distortions are encountered in macrocyclic complexes of Pd(II) and Pt(II) with TAAB (non-planar, saddle-shaped macrocyclic ligand, tetrabenzof[*b,f,j,n*][1,5,9,13]tetraazacyclohexadecine), which have recently been reported to form more highly conducting complexes upon reaction with I_2 [26,27]. The resulting lustrous, metallic, dark red needles exhibit the stoichiometry $[M(TAAB)][I_8]$ where M = palladium(II) or platinum(II). In contrast to the previously discussed complexes only integral oxidation states are involved. As expected from the considerations discussed above, the conductivities are greatly decreased. X-Ray data has confirmed the presence of the octaiodide dianion [28] indicating that the macrocyclic complex has not undergone oxidation, unlike the previously discussed systems (Fig. 4). Within the macrocyclic cation the immediate coordination sphere of the metal is nearly planar; however, the overall geometry of the macrocyclic complex conforms to a hyperbolic paraboloid with cavities of 2.68 \AA about the axial metal sites. The anion consists of discrete Z-shaped non-planar chains of I_8^{2-} composed of two I_3^- units weakly associated with an elongated I_2 . The conductivity in the semiconductor range is thought to occur via macrocycle- I_3^- interactions.

Single-crystal conductivity measurements indicate relatively low conductivities compared to the partially oxidized tetracyanoplatinates and phthalocyanines as shown in Table 4. An interesting effect is observed upon the application of pressure, however. For the Pd-TAAB complex up to 1000-fold increases in conductivity are observed at pressures of 10 kbar as shown in Table 5. Pressure studies of conductivity have been made for some of the unoxidized bis(glyoximates) [29]. Here also a relationship between electrical resistivity and pressure has been noted. Minima in electrical resistivities are found to occur at 193 kbar for bis(dimethylglyoximate)platinum(II). No data was reported for the 0–10 kbar region.

(iv) Spectroscopic investigations

Spectroscopy has played an important role in the investigations of the complexes reported in this paper. IR spectroscopy, resonance Raman scatter-

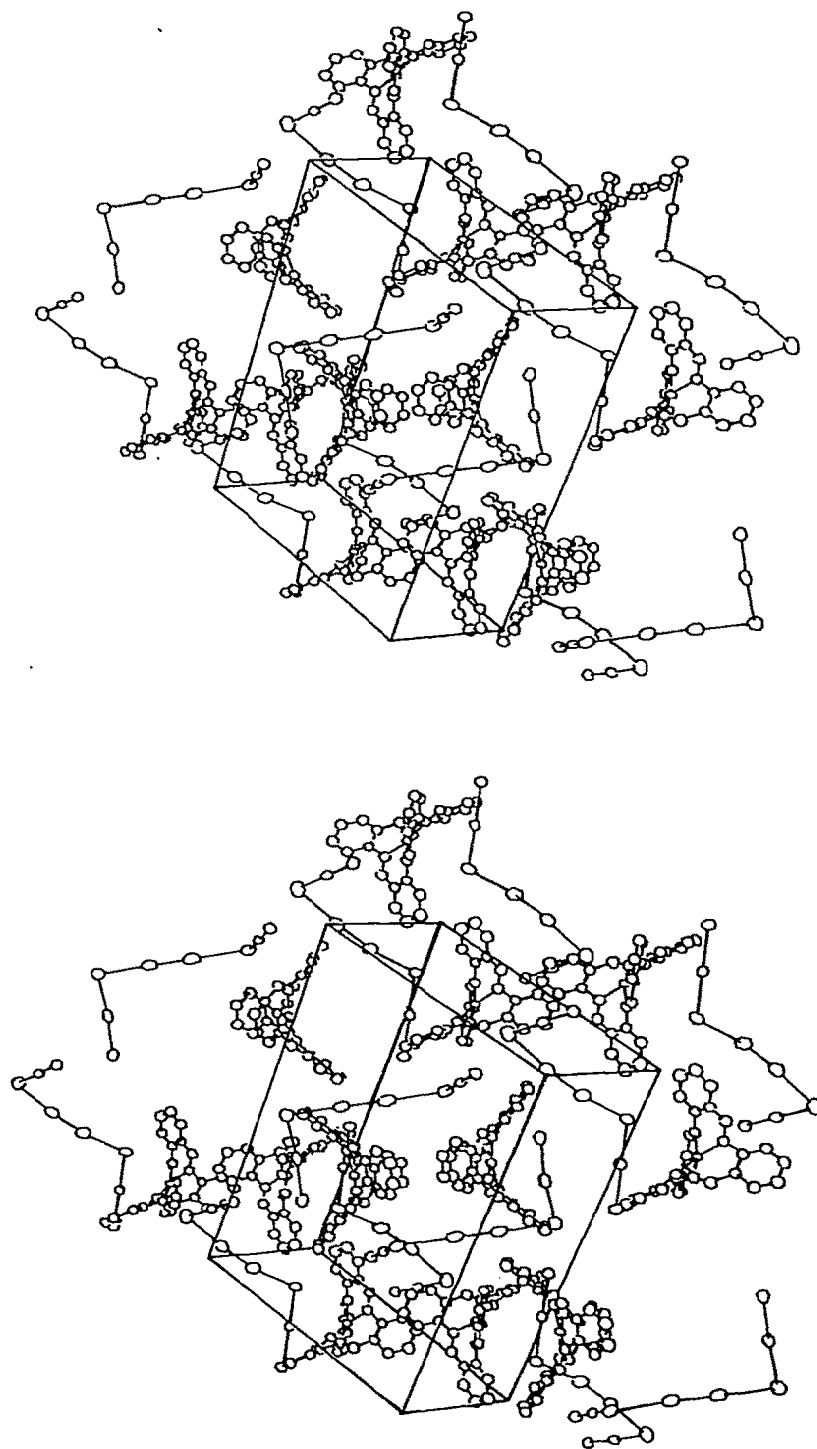


Fig. 4. Packing diagram for Pd(TAAB)(I₈) viewed down the z axis (slightly rotated) with x vertical [28].

TABLE 4

Some physical properties of 1-D conductors

| Conductor | Color | $d(M-M)$ (Å) | Δ^a (Å) | Oxidized σ (ohm cm) ⁻¹ | Non-oxidized σ (ohm cm) ⁻¹ | R^b | Predominant conductive mechanism |
|---|-------------------------|-----------------|-------------------|--|--|------------------|--|
| (1) 1-D tetracyanoplatinates | Bronze, copper, gold | <2.96 | 0.7 | 10 ³ | 10 ⁻⁷ | 10 ¹⁰ | Metal-metal centered |
| Pt-Pt in metal | - | 2.775 | - | 9.4 × 10 ⁴ | - | - | - |
| (2) Planar organometallic (e.g. [NiPc](I ₃) _{0.33}) | Silver-gold | 3.244 | ^c | 1 | 10 ⁻¹¹ | 10 ¹¹ | Ligand-ligand centered |
| Ni-Ni in metal | - | 2.49 | - | 1.46 × 10 ³ | - | - | - |
| (3) Distorted organometallic [e.g. Ni(dpg) ₂ (I ₃) _{0.2}] | Black-gold | 3.22 | 0.32 | 2-11 × 10 ⁻³ | <8 × 10 ⁻⁹ | ~10 ⁷ | Ligand-ligand centered |
| Pd-Pd metal | - | 2.751 | - | 9.26 × 10 ⁴ | - | - | - |

^a $\Delta = d(M-M)(\text{non-oxidized}) - d(MM)(\text{oxidized})$.^b $R = \text{oxidized } \sigma / \text{non-oxidized } \sigma$.^c Comparison meaningless since Ni(Pc) does not stack.

TABLE 5

Conductivity measurements for $M(\text{TAAB})^{n+}$

| Complex | Conductivity ($\Omega^{-1} \text{ cm}^{-1}$) | | | |
|--|--|--------------------|--------------------|---------------------|
| | Single crystal | Powder (1 bar) | Powder (5 kbar) | Powder (10 kbar) |
| $[\text{Pd}(\text{TAAB})][\text{BF}_4]_2$ | — | 1×10^{-9} | 1×10^{-8} | 8×10^{-10} |
| $[\text{Pd}(\text{TAAB})][\text{I}_3]_{2.7}$ | 10^{-7} | 1×10^{-7} | 4×10^{-6} | 5×10^{-5} |
| $[\text{Pt}(\text{TAAB})][\text{BF}_4]_2$ | — | 1×10^{-9} | 1×10^{-7} | 2×10^{-7} |
| $[\text{Pt}(\text{TAAB})][\text{I}_3]_{2.7}$ | 10^{-4} | 6×10^{-7} | 6×10^{-6} | 6×10^{-6} |

ing, Mössbauer, specular reflection techniques, electronic spectroscopy and X-ray photoelectron spectroscopy have all been used in conjunction with X-ray and neutron diffraction methods to characterize these compounds.

(a) Organometallic 1-D tetracyanoplatinates

The first IR spectra of $\text{K}_2\text{Pt}(\text{CN})_4\text{X}_{0.3} \cdot 2.5 \text{ H}_2\text{O}$, where $\text{X} = \text{Cl}, \text{Br}$ were obtained by Krogmann and Hausen [30]. Raman scattering of the CN stretching region for $\text{K}_2\text{Pt}(\text{CN})_4\text{Br}_{0.3} \cdot 3 \text{ H}_2\text{O}$ was measured by Rosseau et al. [31]. From Raman studies, Steigmeier et al. [32] were able to assign two low-frequency vibrations at 21 and 40 cm^{-1} as the TA (transverse acoustical lattice mode) and LA (longitudinal acoustical lattice mode) modes in $\text{K}_{1.75}\text{Pt}(\text{CN})_4 \cdot 1.5 \text{ H}_2\text{O}$. Similar studies of TA and LA modes vs. temperature as measured by IR absorption have been made [33]. Steigmeier et al. [34] also studied $\text{K}_2\text{Pt}(\text{CN})_4\text{Br}_{0.3} \cdot 3 \text{ H}_2\text{O}$ by Raman scattering at 5 and 300 K and found a band at 44 cm^{-1} which has A_1 symmetry, and showed a blue shift as the temperature increased. The cyanide stretching region also was studied as a function of temperature and found to decrease in frequency by 3% and in intensity by 60% from 5 to 300 K. No evidence in Raman scattering was found for the IR band reported at 22 cm^{-1} by Comés et al. [35].

Brüesch and Zeller [36] reported evidence for a Frohlich collective mode at 40 cm^{-1} for $\text{K}_2\text{Pt}(\text{CN})_4\text{Br}_{0.3} \cdot 3 \text{ H}_2\text{O}$. Far-IR transmission and reflection spectra of $\text{K}_2\text{Pt}(\text{CN})_4\text{Br}_{0.3} \cdot 3 \text{ H}_2\text{O}$ were reported by Winterling and Martin [37]. They were able to qualitatively fit a frequency-dependent reflectivity with an oscillator having an LO (longitudinal optical lattice mode) frequency at 52 cm^{-1} .

IR studies of 1-D cation-deficient conductors of the type $\text{M}_{1.75}[\text{Pt}(\text{CN})_4] \cdot 1.5 \text{ H}_2\text{O}$, where $\text{M} = \text{K}, \text{Rb}, \text{Cs}$ were conducted by Ferraro et al. [38]. Figure 5 shows the skeletal modes of vibration for the $\text{Pt}(\text{CN})_4$ moiety of

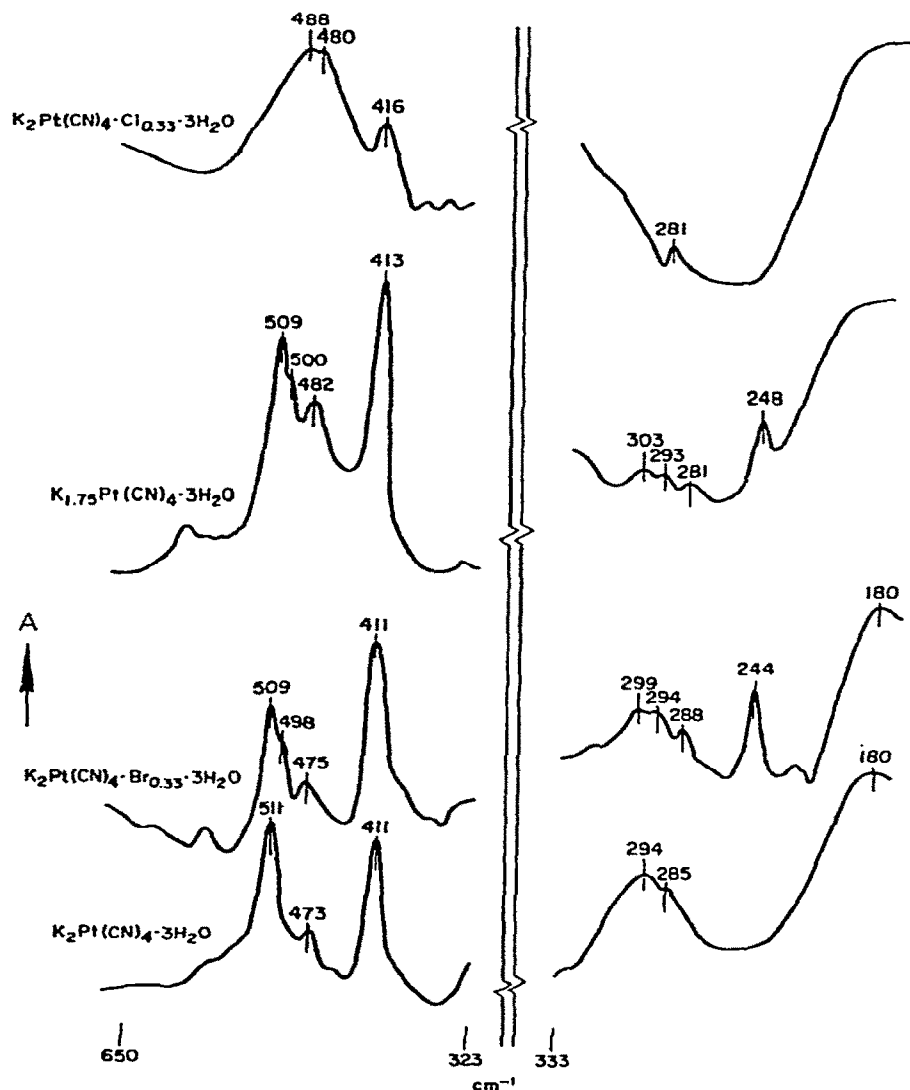


Fig. 5. IR skeletal modes of vibration for the $\text{Pt}(\text{CN})_4$ moiety in tetracyanoplatinate compounds [37].

these complexes. Vibrational studies were made on $\text{K}_2\text{Pt}(\text{CN})_4\text{Br}_{0.3} \cdot 3\text{H}_2\text{O}$ and $\text{K}_2\text{Pt}(\text{CN})_4\text{Cl}_{0.3} \cdot 3\text{H}_2\text{O}$ and the non-centrosymmetric space group obtained from neutron and X-ray diffraction data confirmed [39]. IR data were used to substantiate the presence of the bifluoride ion in 1-D tetracyanoplatinates containing the bifluoride ion [40]. Raman studies of the CN stretching vibrations in 1-D tetracyanoplatinate conductors were made [41]. The A_{1g} and B_{1g} vibrations showed a decrease in frequency as the cation size

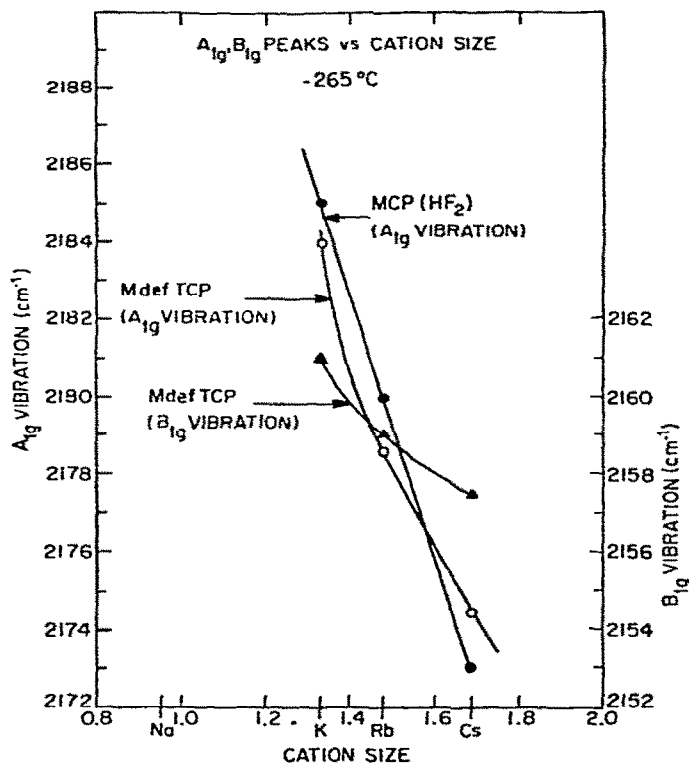


Fig. 6. The A_{1g} and B_{1g} vibration as a function of cation size [40]. Permission granted by the American Institute of Physics and authors.

increased. Figure 6 presents these results.

Finally, to determine and to screen that 1-D metals are synthesized, polarized specular reflectance spectra are used [42]. A 1-D metal shows strong reflection of the polarized light parallel to the chain direction even into the far-IR, while a non-metal shows a maximum and rapid drop-off.

(b) Organometallic complexes

Resonance Raman scattering has played a major role in determining the nature of the geometry of the polyiodides in the complexes discussed in (ii) and (iii) above. Supporting evidence from ^{129}I Mössbauer spectroscopy, ESR and X-ray photoelectron has also been obtained. Whenever X-ray crystallographic data were available, the above notions concerning polyiodide structure were confirmed.

Table 6 summarizes spectroscopic and X-ray data [42–48] for several model compounds containing polyiodides ranging from I_2 to I_{16}^{4-} . The iodine molecule manifests only a Raman spectrum with the symmetrical I–I stretch-

ing vibration occurring at 209 cm^{-1} . The compounds $(\text{C}_6\text{H}_5)_4\text{AsI}_3$ [21] and $(\text{C}_6\text{H}_5\text{CONH}_2)_2\text{HI}_3$ [21,43] show symmetrical I_3^- spectra characterized by a strong band at 114 and 113 cm^{-1} respectively. The X-ray data confirm that all I–I bond distances are equal. For CsI_3 [21], an unsymmetrical I_3^- spectrum is observed, characterized by several vibrations between 99–116 cm^{-1} . Two distinct I–I bond distances are observed. The compound $(\text{CH}_3)_4\text{NI}_5$ has a bent I_5^- geometry $[(\text{I}_2)_2\text{I}]^-$ [44] with Raman bands in the range 158–180 cm^{-1} . The linear chain (trimesic acid $\cdot \text{H}_2\text{O}$) $_{10}\text{HI}_5$ molecule illustrates a main band at 160 cm^{-1} , indicative of the I–I stretching force constant being lowered from that in pure I_2 , due to the redistribution of

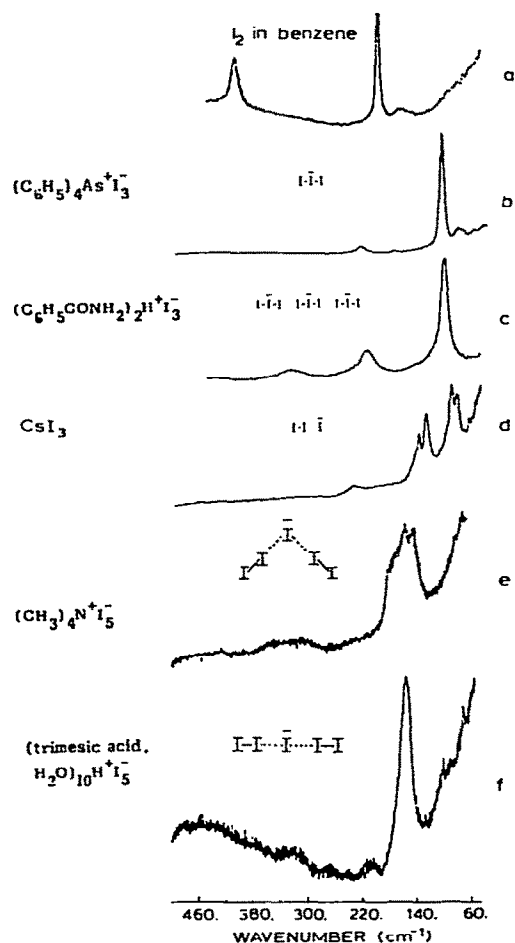
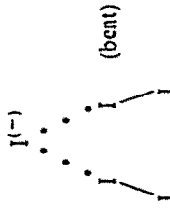
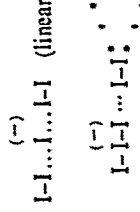
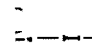
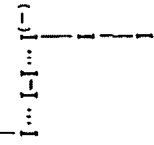
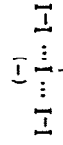

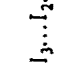


Fig. 7. Resonance Raman spectra of (a) I_2 in benzene solution, (b) $(\text{C}_6\text{H}_5)_4\text{As}^+\text{I}_3^-$ solid, (c) $(\text{C}_6\text{H}_5\text{CONH}_2)_2\text{H}^+\text{I}_3^-$ solid, (d) CsI_3 solid, (e) $(\text{CH}_3)_4\text{N}^+\text{I}_5^-$ solid, (f) (trimesic acid $\cdot \text{H}_2\text{O}$) $_{10}\text{H}^+\text{I}_5^-$ solid.

TABLE 6
Some physical parameters for polyiodide compounds

| Polyiodide anion | Geometry ^a | Compound | Raman data (cm ⁻¹) | IR data (cm ⁻¹) | X-Ray d_{1-1} (Å) | Comments |
|-------------------------------|---|--|---|-----------------------------------|--|---|
| I_2 | I-I | I_2 in benzene | 209 (s) | Not allowed IR spectrum | 2.72 | Only Raman band observed |
| I_3^- | $I-I-I^{(-)}$ (linear, sym) $(-)$ $\dots I-I-I \dots I-I-I \dots$ (chain, sym) | $(C_6H_5)_4As^+I_3^-$ $(C_6H_5CONH_2)_2H^+I_3^-$ | 114 (s) 113 (s) 146 (m), 135 (w) 105 (s), 99 (s) | n.a. ^b n.a. n.a. | 2.92 (equal) 2.92 (all equal) 2.83 3.03 | Typical sym I_3^- spectra Distorted, asym I_3^- spectrum |
| I_5^- (I_2)(I_2) | $I-I-I$ (linear, asym)  | CsI_3 $(CH_3)_4NI_5$ | 108 (sh) 160 (s) I_2 158 (s) | n.a. | 2.93 | Typical I_5^- spectra |
| I_7^- or $I_3(I_2)_2$ | $I-I \dots I \dots I-I$ (linear)  $I-I-I \dots I-I$ (chains) | (trimesic acid $\cdot H_2O$) ₁₀ $H^+I_5^-$ $(C_3H_5)_4NI_7$ | 162 (s) I_2 104 (w-sh) 185 (s) I_2 155 (vw) I_3^- 119 (w) | n.a. n.a. | 2.74 2.735 I_2 2.904 I_3^- | I_2 and I_3^- spectra |

| | | | | |
|--|---|----------------------------------|--------------|---|
| I_8^{4-} |  | 171 (s) I_2 | $2.83^a I_2$ | |
| $I_2(I_3)_2^{2-}$ |  | Cs_2I_8 | n.a. | $2.84, 3.00 I_3^-$ I_2 and I_3^- spectra |
| I_9^- |  | | $2.67 I_2$ | |
| $I_3(I_2)_5^-$ |  | $(CH_3)_4NI_9$ | n.a. | $2.90 I_3^-$ 3.18 |
| I_{16}^{4-} $(I_3)_4(I_2)_2^{4-}$ |  | $(H^+C_7H_8N_4O_2)(I_{16})^{4-}$ | n.a. | $2.76 I_2$ $2.84, 3.03 I_3^-$ |

^a Dotted lines indicate weak interactions of 3.42–3.55 Å.

^b n.a. = not available.

electrons from the iodide ion (I^-) to the two iodine (I_2) units [45]. Other compounds containing moieties like $I_7^- [I_3^-(I_2)_2]$ [46], $I_8^{2-} [I_2(I_3)_2]^{2-}$ [47] show spectra characteristic of a combination of a triiodide ion and iodine molecules, substantiating crystallographic data. No specific data are available for I_9^- [48] and I_{16}^{4-} [49], although by comparison with previous model compounds and bond distances obtained from X-ray data, the geometries $[(I_2)_3I_3]^-$ and $[(I_2)_2(I_3)_4]^{4-}$ are suggested respectively. Figure 7 shows Raman spectra for several of the compounds in Table 6.

By comparing the Raman spectra obtained for the iodine-containing organometallic complexes with the model compounds described above, certain inferences can be made. Figure 8 illustrates several Raman spectra of metal phthalocyanine compounds. Table 7 summarizes Raman data for the organometallic complexes discussed in sections (ii) and (iii) above. The nickel complexes of Pc, OMTB, TBP, bqđ, taa, and tmtaa, as well as the polystannyloxane, polygermyloxane and polysiloxane complexes of Pc, and the palladium and platinum complexes of TAAB all demonstrate a Raman spectrum typical of a triiodide ion. The far-IR data of the latter compounds

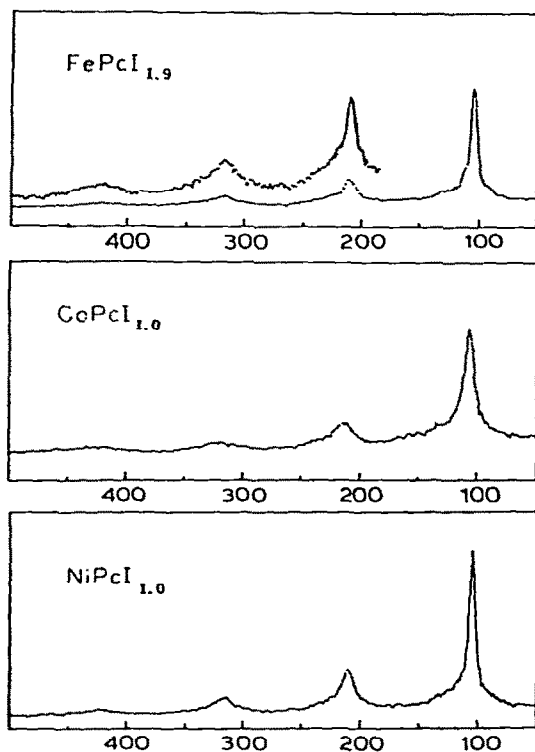


Fig. 8. Resonance Raman spectra of partially oxidized metal phthalocyanine materials with 5145 Å excitation [21]. Permission granted by the N.Y. Academy of Sciences and authors.

were in agreement with the Raman data. However, according to the crystallographic information, an elongated I_2 molecule is also involved in a $[I_2(I_3)_2]^{2-}$ geometry. The Ni and Pd complexes of dpg and the Ni complex of octaethylporphyrin (OEP) demonstrate an I_5^- spectrum $[I_2(I_3)^-]$.

Mössbauer spectroscopy has also complemented the resonance Raman studies. Figure 9 presents typical Mössbauer results for $Ni(dpg)_2(I_5)_{0.2}$ and $Pd(dpg)_2(I_5)_{0.2}$.

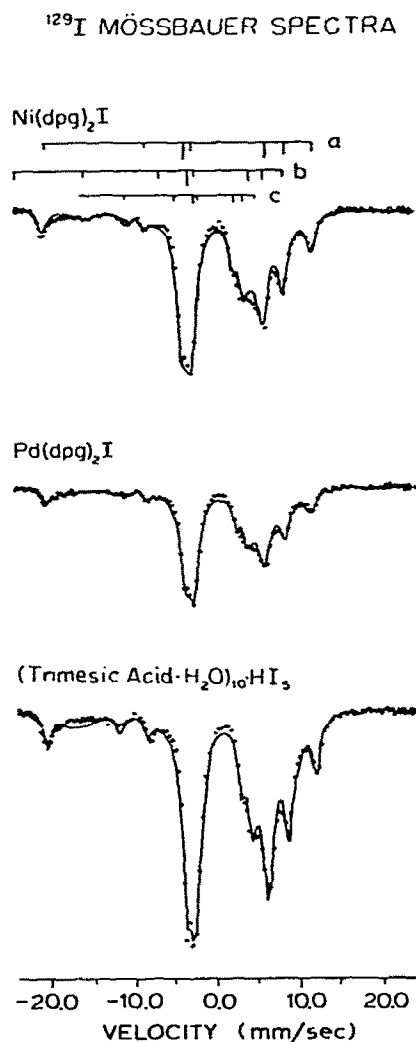


Fig. 9. ^{129}I Mössbauer spectra of several complexes at 4 K. The solid lines represent the best computer fit to data points. Stick figures representing contributing transitions are shown for the $Ni(dpg)_2I$ spectrum. $ZnTe$ is used for the reference of isomer shifts [21]. Permission granted by the N.Y. Academy of Sciences and authors.

TABLE 7

Raman data and geometry of polyiodides in several organometallic complexes

| Metal polyiodide complex | Raman frequency (cm^{-1}) | Geometry of polyiodides |
|---|--------------------------------------|---|
| Ni(Pc)(I ₃) _{0.33} (also Co, Fe) Ni(OMTBP)(I ₃) _{0.36} Ni(OMTBP)(I ₃) _{0.97} Ni(TBP)(I ₃) _{0.33} Ni(bqd) ₂ (I ₃) _{0.17} (also Pd) {[Sn(Pc)O](I ₃) _{0.4} } _n {[Ge(Pc)O](I ₃) _{0.6} } _n {[Si(Pc)O](I ₃) _{0.65} } _n Ni(taa)(I ₃) _{0.6} (also Co, Cu, Pd) Ni(tmtaa)(I ₃) _{0.8} (also Pd) | 107–108 (s) | I ₃ ⁻ |
| Pd(TAAB)(I ₈) ^a | 109 (s) | I ₈ ²⁻ [I ₂ (I ₃) ₂] ²⁻ |
| Ni(OEP)(I ₅) _{0.24} | 167 (s) 113 (sh) | |
| Pd(dpg) ₂ (I ₅) _{0.2} | 160 (vs), 104 (mw) | I ₅ ⁻ [(I ₂)I ₃ ⁻] |
| Ni(dpg) ₂ (I ₅) _{0.2} | 162 (vs), 107 (w) | |

^a Infrared data: 135 (s), 104 (m), 42 (vw).

Although some routine far-IR data were obtained for some of these complexes, only data for Pd(TAAB)I₈ are reported. To what extent Raman and far-IR data are in agreement with the solid-state selection rules for the other complexes remains to be evaluated.

C. SUMMARY

(1) Structural characteristics have been employed to separate square-planar one-dimensional complexes into three classes. The influence of the ligand systems, metal ions, electronic, steric, and valency aspects and their correlation with structure and conductivity have been considered. The compounds all contain partially oxidized species and the classes are as follows: (a) predominantly planar tetracyanoplatinates with close metal-metal spacings; (b) transition metal complexes with extended ligand systems which are still predominantly planar but with longer metal-metal separations; and (c) non-planar complexes with extended ligand systems which, in some instances display even longer intermolecular distances.

(2) Partial oxidation and metal-metal proximity are of equivalent importance. The former would appear to be a prerequisite, while the latter is somewhat more flexible [e.g. Ni(OMTBP)(I₃)_{0.36}].

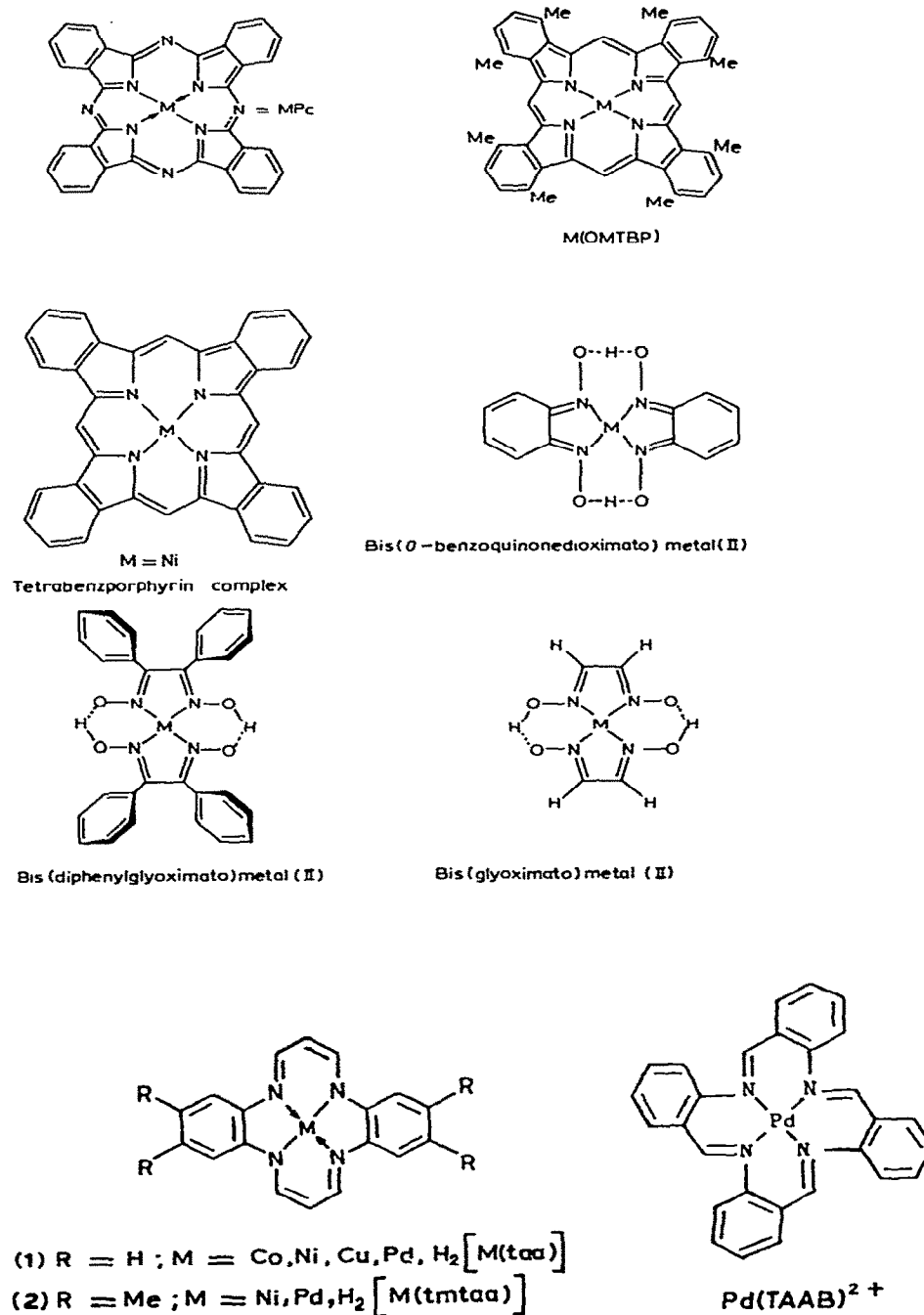


Fig. 10. Structures for various organometallic complexes discussed in this paper.

D. STRUCTURES FOR ORGANOMETALLIC COMPLEXES

The structures of the various organometallic complexes reported in this paper are shown in Fig. 10.

ACKNOWLEDGMENTS

I thank Professor Kristin Bowman Mertes for collaboration on the TAAB work and for her contributions to the first review of this subject [50]. In addition, sincere thanks are in order to Dr. Jack M. Williams, of Argonne National Laboratory, for many valuable discussions on various facets of this review.

Note added in preparation. The use of bromine as a partial oxidant has been investigated by Marks and co-workers. (D.W. Kalina, J.W. Lyding, M.T. Ratajack, C.R. Kannewurf and T.J. Marks, J. Am. Chem. Soc., 102 (1980) 7854). The complexes of brominated nickel and palladium bis(diphenylglyoximates) were prepared. The $M(dpg)_2$ units are in an oxidation state of ca. $+0.20$ ($M=Ni$) and $+0.22$ ($M=Pd$). Resonance Raman spectra show that the bromine is present as the Br_5^- ion, as was found for the iodine analogues [23,24]. The complexes can be formulated as $[Ni(dpg)]_2^{+0.20} [Br_5]_{0.20}^-$ and $[Pd(dpg)]_2^{+0.22} [Br_5]_{0.22}^-$. Conductivities were 9.1×10^{-4} (ohm cm) $^{-1}$ for the Ni compound and 1.5×10^{-4} (ohm cm) $^{-1}$ for the Pd compound.

REFERENCES

- 1 K. Krogmann, Angew. Chem., Int. Ed. Engl., 8 (1969) 35.
- 2 J.S. Miller and A.J. Epstein, Prog. Inorg. Chem., 20 (1976) 1.
- 3 J.L. Peterson, C.S. Schramm, D.R. Stojakovic, B.M. Hoffman and T.J. Marks, J. Am. Chem. Soc., 99 (1977) 286.
- 4 C. Schramm, D.R. Stojakovic, B.M. Hoffman and T.J. Marks, Science, 200 (1978) 47.
- 5 B.M. Hoffman, T.E. Phillips, C.J. Schramm and S.K. Wright, in W.E. Hatfield (Ed.), Molecular Metals, Plenum Press, New York, 1979, p. 393.
- 6 J.S. Miller and C.H. Griffiths, J. Am. Chem. Soc., 99 (1977) 749.
- 7 L.F. Mehne and B.B. Wayland, Inorg. Chem., 14 (1975) 881.
- 8 H.J. Keller and K. Siebold, J. Am. Chem. Soc., 93 (1971) 1309.
- 9 A.S. Foust and R. Soderberg, J. Am. Chem. Soc., 89 (1967) 5507.
- 10 A.E. Underhill, D.M. Watkins and R. Pethig, Inorg. Nucl. Chem. Lett., 9 (1973) 1269.
- 11 J.J. Andre, A. Buber and F. Gaut, Ann. Phys. (Paris), 1 (1976) 145.
- 12 Z.G. Soos and D.J. Klein, in R. Foster (Ed.), Molecular Association, Academic Press, New York, 1975, Vol. 1, pp. 1-119.
- 13 J.B. Torrance, in H.J. Keller (Ed.), Chemistry and Physics of One-Dimensional Metals, Plenum Press, New York, 1977.
- 14 J.M. Williams and A.J. Schultz, Ann. N.Y. Acad. Sci., 313 (1978) 509.
- 15 T.E. Phillips and B.M. Hoffman, J. Am. Chem. Soc., 99 (1977) 7734.
- 16 T.E. Phillips, R.P. Scaringe, B.M. Hoffman and J.A. Ibers, J. Am. Chem. Soc., 102 (1980) 3435.

- 17 J.M. Williams and A.J. Schultz, in W.E. Hatfield (Ed.), *Molecular Metals*, Plenum Press, New York, 1979, pp. 337–368.
- 18 A.J. Schultz, C.C. Coffey, G.C. Lee and J.M. Williams, *Inorg. Chem.*, 16 (1977) 2129.
- 19 R.K. Brown and J.M. Williams, *Inorg. Chem.*, 17 (1978) 2607.
- 20 J.M. Williams, A.J. Schultz, A.E. Underhill and K. Carneiro, in J.S. Miller (Ed.), *Extended Linear Chain Compounds*, Plenum Press, New York, in press, and references therein.
- 21 (a) T.J. Marks, *Ann. N.Y. Acad. Sci.*, 313 (1978) 594.
(b) C.J. Schramm, R.P. Scaringe, D.R. Stojakovic, B.M. Hoffmann, J.A. Ibers and T.J. Marks, *J. Am. Chem. Soc.*, 102 (1980) 6702.
- 22 K.F. Schoch, Jr., B.R. Kundalkar and T.J. Marks, *J. Am. Chem. Soc.*, 101 (1979) 7071.
- 23 M. Cowie, A. Gleizes, G.W. Grynkewich, D.W. Kalina, M.S. McClure, R.P. Scaringe, R.C. Teitelbaum, S.L. Ruby, J.A. Ibers, C.R. Kannewurf and T.J. Marks, *J. Am. Chem. Soc.*, 101 (1979) 2921.
- 24 A. Gleizes, T.J. Marks and J.A. Ibers, *J. Am. Chem. Soc.*, 97 (1975) 3545.
- 25 (a) L.D. Brown, D.W. Kalina, M.S. McClure, S. Schultz, S.L. Ruby, J.A. Ibers, C.R. Kannewurf and T.J. Marks, *J. Am. Chem. Soc.*, 101 (1979) 2937.
(b) L.S. Lin, T.J. Marks, C.R. Kannewurf, J.W. Lyding, M.S. McClure, M.T. Ratajack and T. Whang, *J. Chem. Soc., Chem. Commun.*, (1980) 954.
- 26 K.B. Mertes and J.R. Ferraro, *J. Chem. Phys.*, 70 (1979) 646.
- 27 A.J. Jircitano, M.D. Timken, K.B. Mertes and J.R. Ferraro, *J. Am. Chem. Soc.*, 101 (1979) 7661.
- 28 A.J. Jircitano, M.C. Colton and K.B. Mertes, *Inorg. Chem.*, 20 (1981) 890.
- 29 A. Onodera, I. Shirotani, Y. Hara and H. Anzai, in R.D. Timmerhaus and M.S. Barber (Eds.), *High-Pressure Science and Technology*, Plenum Press, New York, 1979, Vol. 1., p. 498.
- 30 K. Krogmann and H.D. Hausen, *Z. Anorg. Allg. Chem.*, 358 (1968) 67.
- 31 D.L. Rousseau, M.A. Butler and H.J. Guggenheim, *Phys. Rev. B*, 10 (1974) 2281.
- 32 E.F. Steigmeier, D. Baeriswyl, H. Auderset and J.M. Williams, in S. Darisic et al. (Eds.), *Quasi 1-D Conductors, (II)*, Springer-Verlag, Berlin, 1979, pp. 229–238.
- 33 P. Brüesch, S. Strässler and H.F. Zeller, *Phys. Rev. B*, 12 (1975) 219.
- 34 E.F. Steigmeier, R. Loudon, G. Harbeke, H. Auderset and G. Scheiber, *Solid. State Commun.*, 17 (1975) 1447.
- 35 R. Comés, B. Renken, L. Pintschovius, R. Currat, W. Gläser and G. Scheiber, *Phys. Status Solidi B*, 71 (1975) 171.
- 36 P. Brüesch and H.R. Zeller, *Solid State Commun.*, 14 (1974) 1037.
- 37 G. Winterling and T.P. Martin, in H.G. Schuster (Ed.), *One Dimensional Conductors*, Springer-Verlag, Berlin, 34 (1975) 244.
- 38 J.R. Ferraro, L.J. Basile and J.M. Williams, *J. Chem. Phys.*, 67 (1977) 742.
- 39 J.R. Ferraro, L.J. Basile and J.M. Williams, *J. Chem. Phys.*, 64 (1976) 732.
- 40 L.J. Basile, J.R. Ferraro and J.M. Williams, *J. Chem. Phys.*, 66 (1977) 4941.
- 41 J.R. Ferraro, L.J. Basile, J.M. Williams, J.I. McOmber, D.F. Shriver and D.R. Breig, *J. Chem. Phys.*, 69 (1978) 3871.
- 42 K. Krogmann and H.P. Geserich, in L.V. Interrante (Ed.), *Extended Interactions Between Metal Ions in Transition Metal Complexes*, *Am. Chem. Soc. Symp.*, Ser. No. 5, 1974, 350 pp.
- 43 J.M. Reddym, K. Knox and M.B. Robin, *J. Chem. Phys.*, 40 (1964) 1082.
- 44 J. Runsink, S. Swen-Walstra and T. Mighelsen, *Acta Crystallogr., Sect. B*, 28, (1972) 1331.

- 45 F.H. Herbstein and M. Kapon, *Acta Crystallogr., Sect. A*, 28 (1972) S74.
- 46 E.E. Havinga and E.H. Wiebenga, *Acta Crystallogr.*, 11 (1958) 733.
- 47 W.J. James, R.J. Hach, D. French and R.E. Rundle, *Acta Crystallogr.*, 8 (1955) 814.
- 48 E.E. Havinga, K.H. Boswijk and E.H. Wiebenga, *Acta Crystallogr.*, 7 (1954) 487.
- 49 F.H. Herbstein and M.J. Kapon, *J. Chem. Soc., Chem. Commun.*, (1975) 677.
- 50 J.R. Ferraro and K.B. Mertes, *J. Coord. Chem.*, 36 (1981) 357.